

Dynamic and Transient Analysis of Power Distribution Systems With Fuel Cells—Part I: Fuel-Cell Dynamic Model

Kourosh Sedghisigarchi, *Student Member, IEEE*, and Ali Feliachi, *Senior Member, IEEE*

Abstract—The first part of this two-part-paper develops a comprehensive nonlinear dynamic model of a solid-oxide fuel cell (SOFC) that can be used for dynamic and transient stability studies. The model based on electrochemical and thermal equations, accounts for temperature dynamics and output voltage losses. The output voltage response of a stand-alone fuel-cell plant to a step load change, a fuel flow step change, and fast load variations are simulated to illustrate the dynamic behavior of SOFC for fast and slow perturbations. A method for interfacing the proposed fuel-cell models to a power system stability package is developed.

Index Terms—Distributed generation, dynamic modeling, fuel cell, transient stability.

I. INTRODUCTION

DISTRIBUTED generation is expected to play a major role in the electric power production of the future. Most likely, fuel cells and microturbines will be the dominant grid-connected distributed generators (DGs). Moreover, fuel cells are attractive because they are modular, efficient, and environmentally friendly. However, fuel cells are dynamic devices which will affect the dynamic behavior of the power system to which they are connected. Analysis of such a behavior requires an accurate dynamic model, such as the one proposed in this paper.

Two types of fuel cells are likely to be used as power plants namely solid-oxide fuel cells (SOFCs) and molten carbonate fuel cells (MCFCs) [1]. Each has a specific dynamic model. Most of the published models, however, concentrate on stand-alone fuel cells. Padullés, Ault, McDonald [2] develop a SOFC model which includes species dynamics, but it does not consider temperature dynamics. Hall and Colclaser [3] modeled a 3-kW SOFC but they did not take into account dynamics of the chemical species. Achenbach develops a mathematical model of a planar SOFC, which concentrates on effects of temperature changes on output voltage response [4]. Temperature dynamics is modeled in a three-dimensional (3-D) vector space. The same author investigated the transient behavior of a stand-alone SOFC caused by a load change in [5]. It shows that the relaxation time

of the output voltage is highly related to the effect of temperature dynamics.

Standalone MCFC dynamic models are presented in [5], [6], [12]. These models are accurate and detailed. However, MCFC internal chemical reactions are different from SOFCs, resulting in different dynamic models.

The model proposed in this paper includes the electrochemical and thermal aspects of chemical reactions inside the fuel-cell stack (i.e., temperature and chemical species dynamics are considered). Furthermore, voltage losses due to ohmic, activation, and concentration losses are accounted for. Therefore, this SOFC model complements existing models such as the ones developed in [2]–[5], [12]. The model is suitable for both small-signal and transient stability studies.

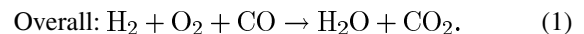
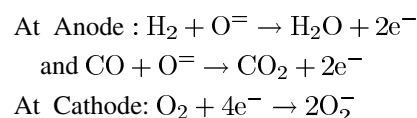
Fuel cells are dc voltage sources connected to electric power networks through dc/ac inverters. A method to connect the proposed SOFC model to a power network through an interface block is presented. The fuel-cell model and its interface block are implemented in MATLAB and incorporated with a power system stability analysis package called the power analysis toolbox (PAT) [14].

The paper is organized as follows: in Section II, general principles of SOFC are explained. Fuel-cell dynamic modeling is described in Section III. Simulation results for stand-alone fuel cell are shown in Section IV. Section V investigates a method for connection to grid.

II. SOLID-OXIDE FUEL-CELL GENERAL PRINCIPLES

A. Principles of SOFC

A typical arrangement of an autonomous fuel-cell power plant is shown in Fig. 1, along with its major chemical reactions. The chemical reactions inside the cell that are directly involved in the production of electricity are [3]



The anode is typically a porous nickel-zirconia cermet that serves as the electrocatalyst, which can be electronically conductive. It allows fuel gas to reach the electrolyte interface, and catalyzes the fuel oxidation reaction.

Manuscript received March 31, 2003. This work was sponsored in part by the National Science Foundation under Grant ECS-9870041 and in part by a US DOE/EPSCoR WV State Implementation Award.

The authors are with the Lane Department of Computer Science and Electrical Engineering, West Virginia University, Morgantown, WV 26506-6109 USA (e-mail: kourosh@csee.wvu.edu; alfeliachi@mail.wvu.edu).

Digital Object Identifier 10.1109/TEC.2004.827039

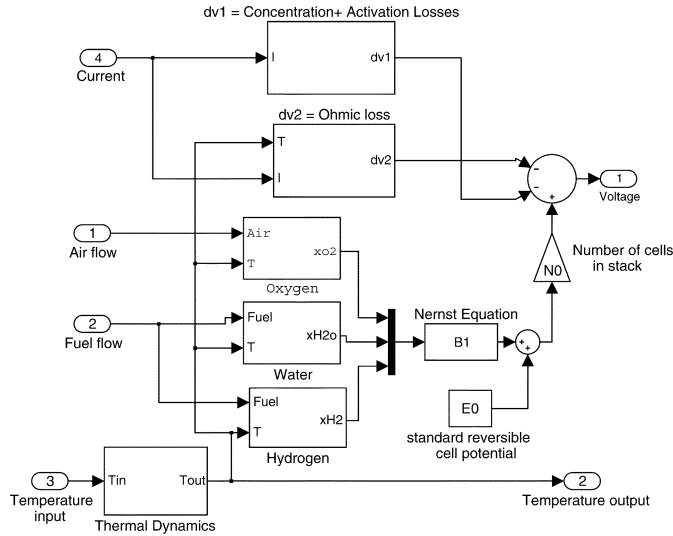


Fig. 1. Dynamic model of SOFC developed in MATLAB/SIMULINK.

B. SOFC Features

The operating temperature is in the range of 900–1000 °C and the electrical efficiency is 50–60%. The proposed stack model is based on the following assumptions.

- 1) Stack is fed with hydrogen and air (fuel processor dynamic is not included)
- 2) A uniform gas distribution among cells is assumed, since there is a small deviation of the gas distribution among the cells.
- 3) Based on the uniform gas distribution, there is no heat transfer among cells. Each cell has the same temperature and current density [2].
- 4) The ratio of pressures between the interior and exterior of the channel is large enough to consider that orifice choked [2], [8].

III. SOFC DYNAMIC MODEL

The proposed dynamic model is based on the following chemical and physical principles:

- 1) electrochemical model: Component material balance equations;
- 2) thermal model: Energy balance equations;
- 3) voltage activation, concentration, and ohmic losses: Nernst voltage equation.

These components are described below.

A. Component Material Balance Equation

The change in concentration of each specie that appears in the above chemical reactions can be written in terms of input and output flow rates and exit molarity (x_i) due to the following chemical reaction [6], [11]:

$$\frac{PV}{RT} \frac{d}{dt} x_i = N_i^{\text{in}} - N_i^{\text{o}} + N_i^r. \quad (2)$$

where

- V compartment volume (m^3);
- $N_i^{\text{in}}, N_i^{\text{o}}$ Molar flow rates (mole/s) of the i th reactant at the cell input and output (exit), respectively;

- N_i^r reaction rate (mole/s) of the i th reactant;
- T cell temperature in °K;
- P cell pressure (atm);
- R gas constant (8.31 J/mole °K).

The cell utilization (u) is defined through the input and output hydrogen flow rates (N_{H_2}) as follows:

$$u = \frac{N_{\text{H}_2}^{\text{in}} - N_{\text{H}_2}^{\text{o}}}{N_{\text{H}_2}^{\text{in}}}. \quad (3)$$

For orifice that is choked [8], molar flow of any gas through the valve is proportional to its partial pressure inside the channel according to the following expressions [2]:

$$\frac{N_{\text{H}_2}}{x_{\text{H}_2}} = K_{\text{H}_2} \quad \frac{N_{\text{H}_2\text{o}}}{x_{\text{H}_2\text{o}}} = K_{\text{H}_2\text{o}} \quad (4)$$

where

- N_{H_2} hydrogen flow that reacts (kmol/s);
- K_i valve molar constants;
- x_i mole fractions of species.

Applying the Laplace transformation to the above equations and isolating the hydrogen partial pressure, yields the following expressions:

$$x_{\text{H}_2}(s) = \frac{\frac{1}{K_{\text{H}_2}}}{1 + \tau_{\text{H}_2}s} (N_{\text{H}_2}^{\text{in}} - 2K_r I) \quad (5)$$

$$\tau_{\text{H}_2} = \frac{V}{K_{\text{H}_2}RT} \quad (6)$$

where τ_{H_2} , expressed in seconds, is the time constant associated with the hydrogen flow and is a function of temperature.

K_r is a constant dependent on Faraday's constant and number of electrons (N) in the reaction

$$K_r = \frac{N}{4F}. \quad (7)$$

Fig. 12 given in the Appendix shows the hydrogen block developed in MATLAB based on (5) and (6). Oxygen and water blocks have a similar structure as the hydrogen block.

B. Energy Balance Equation

The fuel-cell power output is closely related to the temperature of the cell unit. The heat storage in the thin fuel unit gas or oxidant gas layer is neglected. The thin fuel unit or oxidant gas layers are lumped to the cell unit and gas layers are assumed to have the same temperature as the cell unit [3]–[5], [12].

The energy balance equation for each cell unit is as follows:

$$M_p C_p \frac{dT}{dt} = q_e V_e + \sum Q_i \quad (8)$$

where

- M_p mass of the cell unit (in kilograms);
- V_e volume of the cell unit (m^3);
- C_p heat capacity of the cell unit (in Joules per kilogram.Kelvin);
- T temperature of the cell unit (in Kelvin);
- q_e heat generated from the electrochemical reaction per volume unit;
- Q_i total heat (J) which is the summation of the q_s and other conductive, convective, and radiative heat between cell unit and separators [4], [5], [11], [12].

Stack temperature equations are based on [4], [5], and [14]. Details of thermal dynamics block of Fig. 1 are shown in the Appendix (Fig. 11).

C. Nernst's Voltage Equation

Applying Nernst's equation and Ohm's law (taking into account ohmic, concentration, and activation losses), the stack output voltage is represented as follows [6], [7], [11], [12]:

$$V_{dc} = V_o - rI - \eta_{act} - \eta_{con} \quad (9)$$

$$V_o = N_o \left(E^o + \frac{RT^o}{2F} \ln \frac{x_{H_2} x_{O_2}^{1/2}}{x_{H_2O}} \right) \quad (10)$$

where

V_o	open-circuit reversible potential (in volts);
E^o	standard reversible cell potential;
x_i	mole fraction of species;
r	ohmic resistance (in ohms);
F	Faraday's constant (Coulomb per kilomole);
T	stack temperature (in Kelvin);
N_o	number of cells in stack;
η_{act}	activation losses (in volts);
η_{con}	concentration losses (in volts);
I	stack current (in amps).

Block B1 in Fig. 1 is Nernst's equation part of the dynamic model.

1) *Concentration Losses*: As the reactant is consumed at the electrode by electrochemical reaction, there is a loss of potential due to the inability of the surrounding material to maintain the initial concentration of the bulk fluid. Concentration loss equation is as follows [3], [6], [7], [10]–[12]:

$$\eta_{con} = \frac{RT}{n_a F} \ln \left(1 - \frac{i}{i_L} \right) \quad (11)$$

where i is the stack current, i_L is the limiting current, and n_a is the number of electrons participating in the reaction.

2) *Activation Losses*: Activation polarization is present when the rate of an electrochemical reaction at an electrode surface is controlled by sluggish electrode kinetics [7], [11], [12]. Activation loss equation is as follows:

$$\eta_{act} = \frac{RT}{\alpha nF} \log \left(\frac{i}{i_0} \right) \quad (12)$$

where α is the electron transfer coefficient of the reaction at the electrode being and i_0 is the exchange current density. Voltage drop due to the activation loss can be expressed by a semi-empirical equation, called the Tafel equation as follows:

$$\eta_{act} = a + b \log i \quad (13)$$

where $a = (-2.3RT/\alpha nF) \log i_0$ and $b = 2.3RT/\alpha nF$ are called Tafel constant and Tafel slope, respectively. A plot of electrode potential versus the logarithm of current density is called the "Tafel plot" and the resulting straight line is the "Tafel line." The Tafel slope for an electrochemical reaction is about 110 mV/decade at room temperature. A tenfold increase in current density results in a 110-mV increase in the activation polarization [11].

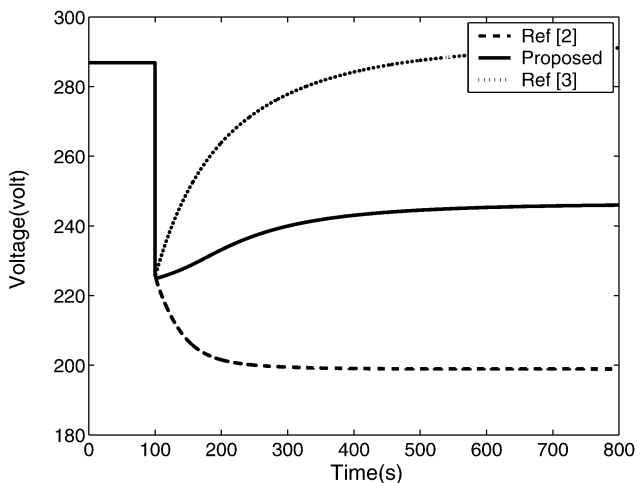


Fig. 2. Output stack voltage response due to stack current step increase.

3) *Ohmic Resistance*: Ohmic losses occur because of resistance to the flow of ions in the electrolyte and resistance to flow of electrons through the electrode materials. This resistance is dependent on the cell temperature and is obtained by [7] and [12]

$$r = \alpha \exp \left[\beta \left(\frac{1}{T_o} - \frac{1}{T} \right) \right] \quad (14)$$

where T is the stack temperature and α, β are constant coefficients. The Laplace transform of the above equations yields the desired dynamic state space components shown in Fig. 1. Details of ohmic, concentration, and activation losses blocks are shown in Figs. 9 and 10 given in the Appendix.

IV. STAND-ALONE FUEL-CELL SIMULATIONS

In this section, the output voltage response of a stand-alone 100-kW solid-oxide fuel cell to slow and fast load variation is presented. This SOFC is connected to a resistive load. The steady-state data for this fuel cell are given in the Appendix.

First, a step change in the stack current (from 300 to 500 A) is applied. The output voltage is shown by a solid line in Fig. 2. The result obtained is compared to responses using other SOFC models given in [2], [3]. By removing the species and temperature dynamic blocks from the proposed model, the dashed and dotted lines of Fig. 3 are obtained. They are similar to the responses given in [2] and [3].

In this simulation, input air and fuel flows are assumed constant. The difference between the outputs is due to species dynamics, which were neglected in [3] and temperature dynamics, which were ignored in [2]. The response from the proposed model is similar to the one given in [12] for a 1-MW MCFC.

The conclusion is that temperature dynamics, species dynamics, and voltage losses should be included in the modeling for slow time frames. In addition, in this case, the cell temperature varies from 1000 to 1400 °K as shown in Fig. 3. The temperature takes 800 s to reach the new steady-state value.

Second, the voltage step response of the SOFC due to the change in fuel flow input from 1.2 to 1.6 kmol/s is shown in Fig. 4. This shows that the output voltage takes more than 150 s to reach a new steady-state value.

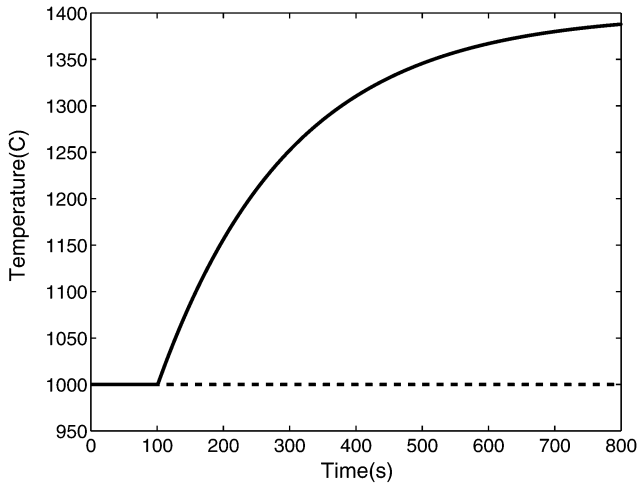


Fig. 3. Output stack temperature response due to stack current step increase.

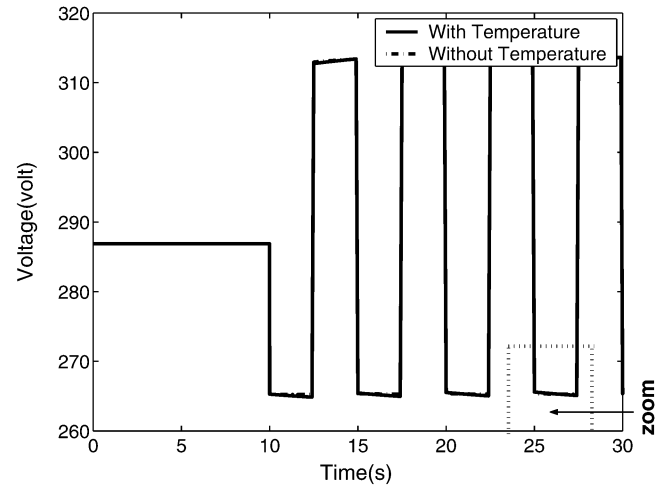


Fig. 5. Output stack voltage response with/without temperature variations.

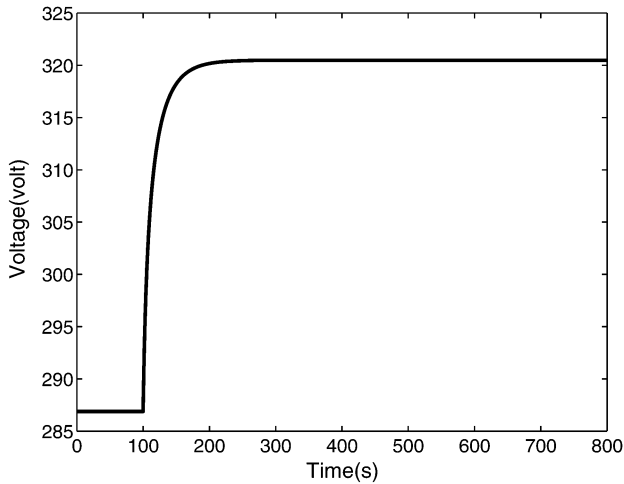


Fig. 4. Output voltage response due to fuel flow step change.

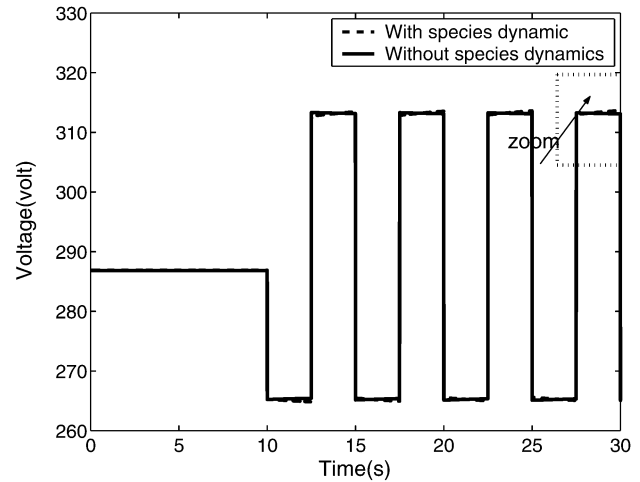


Fig. 6. Output voltage response with/without species dynamics consideration.

Third, the output voltage of the fuel cell with fast resistive load variations is shown in Fig. 5. In this case, the input fuel flow is constant. Here, the dc voltage is affected by temperature dynamics, but not by much, as shown in Fig. 5. Hence, temperature dynamics can be neglected for short time intervals.

Finally, the effects of species dynamics are shown in Fig. 6. It is concluded that species dynamics can be neglected for short time intervals. Fig. 7(a) and (b) show zoom areas of Figs. 5 and 6, respectively.

This section demonstrates that temperature and species dynamics are important for slow transients. The proposed model confirms that these dynamics can be neglected for fast transients [3].

V. CONNECTING FUEL CELL TO THE GRID

To simulate a power system that contains a fuel cell, the model developed earlier needs to be incorporated into a power system stability package, which in this case is the MATLAB based power analysis toolbox (PAT) developed at the Advanced Power Engineering Research Center at West Virginia University [14]. The interface block and initialization procedure required are described next.

Fuel-cell power plants are connected to the grid by a power-conditioning unit (PCU). Applying pulse-width-modulation (PWM) technique to a GTO-based voltage-source converter (VSC) allows representation of the fuel cell with a voltage at fundamental frequency. The injected voltage is given by [9] and [14]

$$\vec{V}_{ac} = m \cdot V_{dc} \cdot \angle \delta = V_{ac} \angle \delta \quad (15)$$

$$I_{dc} = m \cdot I_{ac} \cdot \cos(\phi) \quad (16)$$

where m is the amplitude modulation index of the converter and ϕ is the angle between \vec{V}_{ac} , \vec{I}_{ac} . The voltage magnitude V and the firing angle ψ are controllable in the range of $V^{\min} < V < V^{\max}$ and $0 < \psi < 360^\circ$.

A. Load Flow and Initialization

Initialization of a power system stability program requires a load-flow solution to establish the initial conditions. For load-flow calculations, fuel cell is considered as a generator bus (PV bus) where P and V_F (shown in Fig. 8) are specified.

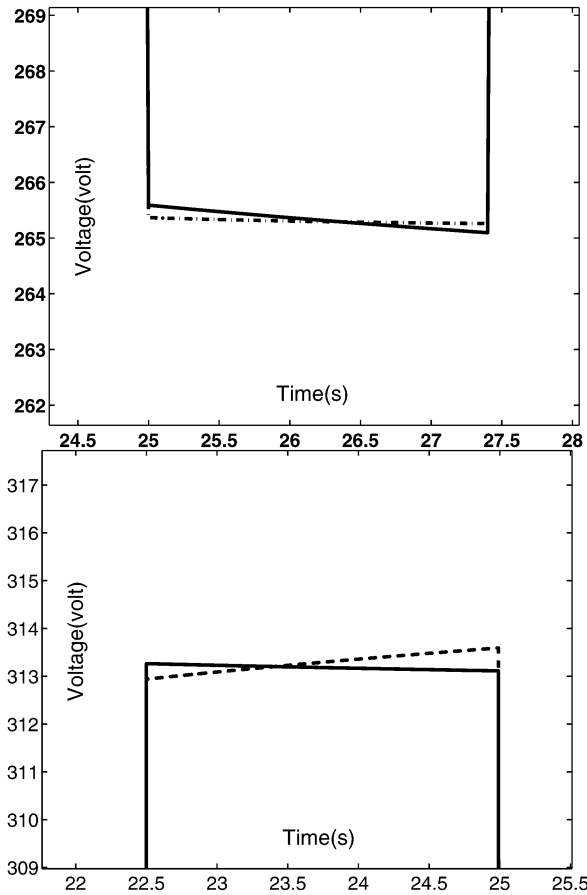


Fig. 7. (a) Zoom plot of Fig. 5. (b) Zoom plot of Fig. 6.

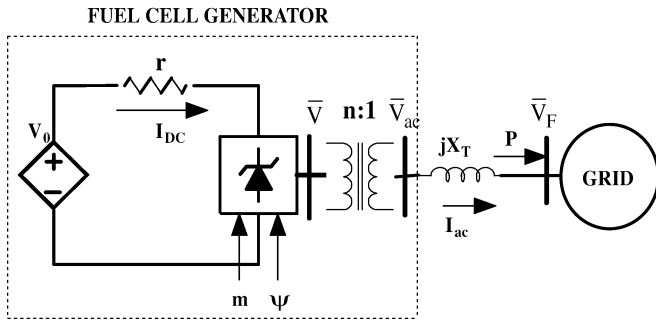


Fig. 8. Fuel cell connected to grid.

Once a standard load-flow problem has been solved, then the internal values can be computed as follows:

$$\bar{I}_{ac} = \frac{P - jQ}{\bar{V}_F^*} \quad (17)$$

$$\bar{V}_{ac} = \bar{V}_F + jX_T \bar{I}_{ac} \quad (18)$$

$$\bar{V}_{ac} = V_{ac} \angle \delta \quad (19)$$

$$\psi = \delta - \delta_F. \quad (20)$$

 TABLE I
 FUEL-CELL OPERATING POINT DATA

Rated power	100 kW
Rated stack voltage	286.3V
Rated stack current	300 A
Number of cells	384
Number of stacks	1
Open circuit voltage for each cell	0.935 V
Input fuel flow (Fuel)	1.2e-3 kmol/s
Input air flow (Air)	2.4e-3 kmol/s
Tafel slope(b)	0.11
Tafel constant (a)	0.05
Cell area	1000cm ²
Operating point cell temperature (TH2)	1000° C
Ohmic resistance constant (β)	-2870
Ohmic resistance constant (α)	0.2
Constant temperature (T0)	923° C
Thickness (b_{ref})	5 mm
Thermal conductivity (l_s)	15 W/ (m K)
Efficiency (η)	80%
Density (ρ_0)	7000 kg/m ³
Limiting current (i_L)	0.8 A/m ²
KH2	8.43e-4 kmol/(atm s)

Using

$$V_{dc} = \frac{2\sqrt{2}nV_{ac}V_B}{m} \quad (21)$$

where n is the transformer turn ratio, m is the modulation index, and V_B is the system-side base voltage. Also

$$P = V_{dc} \cdot I_{dc} \quad (22)$$

where V_{dc} is defined in (9). The three above equations yield the values of m , I_{dc} , and V_{dc} .

The other internal parameters such as operating point stack current, molar fraction of species are calculated using the dynamic model described in Section III.

B. Interface Block for Transient Behavior

The load-flow equations of a power system that contains a fuel cell and generators with internal voltages \bar{E}_G are written in matrix form as

$$\begin{bmatrix} \bar{I}_F \\ \bar{I}_G \end{bmatrix} = \begin{bmatrix} Y_{FF} & Y_{FG} \\ Y_{GF} & Y_{GG} \end{bmatrix} \begin{bmatrix} \bar{V}_F \\ \bar{E}_G \end{bmatrix} \quad (23)$$

$$\bar{I}_F = \bar{I}_{ac} = \frac{\bar{V}_{ac} - \bar{V}_F}{jX_T} = Y_{FG}\bar{E}_G + Y_{FF}\bar{V}_F \quad (24)$$

which (23) can be expressed as

$$\bar{V}_F = L_G \bar{E}_G + L \bar{V}_{ac} \quad (25)$$

where

$$L_G = \left(\frac{-1}{jX_T} - Y_{FF} \right)^{-1} Y_{FG} \quad (26)$$

$$L = - \left(\frac{-1}{jX_T} - Y_{FF} \right)^{-1} \frac{1}{jX_T}. \quad (27)$$

In which Y_{FF} is the admittance matrix connecting the fuel-cell output ac current to the voltage at the fuel-cell bus and Y_{FG} is the admittance matrix connecting the fuel-cell output ac current in terms of generator internal voltages.

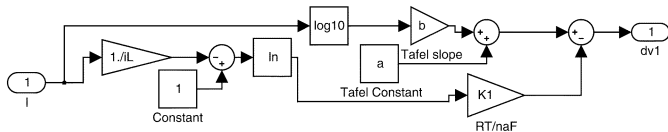


Fig. 9. Concentration and activation loss block of SOFC model.

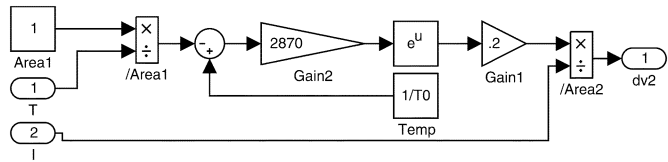


Fig. 10. Ohmic loss subsystem of SOFC dynamic block.

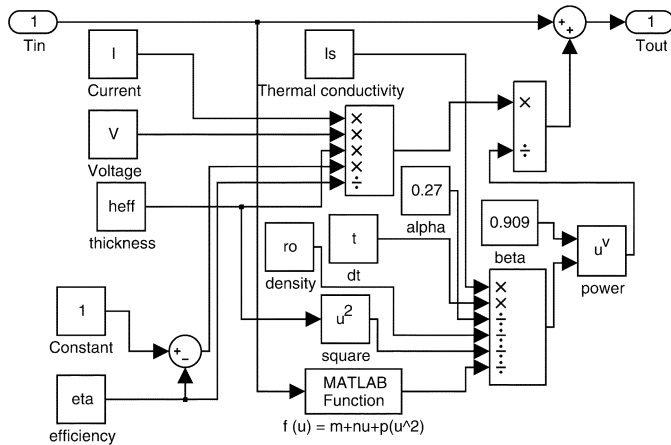


Fig. 11. Thermal dynamic block of SOFC model.

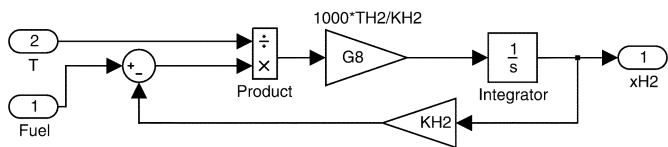


Fig. 12. Hydrogen subsystem of SOFC developed in MATLAB/SIMULINK.

VI. CONCLUSION

This paper describes a detailed dynamic model of a solid-oxide fuel cell (SOFC), which can be used for small signal and transient stability studies. The model based on electrochemical and thermal equations accounts for temperature dynamics and output voltage losses.

Simulation of a stand-alone SOFC shows that stack temperature dynamics plays an important role in dc output voltage level. Simulation results show that for very fast load variations, temperature and species dynamic can be ignored.

Also in this paper, a method to connect the proposed fuel-cell model to a power stability package, namely the power analysis toolbox (PAT), a MATLAB-based toolbox, has been developed.

APPENDIX

See Figs. 9–12 and Table I.

REFERENCES

- [1] R. Anahara, S. Yokokawa, and M. Sakurai, "Present status and future prospects for fuel cell power systems," *Proc. IEEE*, vol. 81, pp. 399–408, Mar. 1993.
- [2] J. Padullés, G. W. Ault, and J. R. McDonald, "An integrated SOFC plant dynamic model for power system simulation," *J. Power Sources*, pp. 495–500, 2000.
- [3] D. J. Hall and R. G. Colclaser, "Transient modeling and simulation of tubular solid oxide fuel cells," *IEEE Trans. Energy Conversion*, vol. 14, pp. 749–753, Sept. 1999.
- [4] E. Achenbach, "Three-dimensional and time-dependent simulation of a planar SOFC stack," *J. Power Sources*, vol. 49, 1994.
- [5] —, "Response of a solid oxide fuel cell to load change," *J. Power Sources*, vol. 57, pp. 105–109, 1995.
- [6] M. D. Lukas, K. Y. Lee, and H. Ghezel-Ayagh, "Development of a stack simulation model for control study on direct reforming molten carbonate fuel cell power plant," *IEEE Trans. Energy Conversion*, vol. 14, pp. 1651–1657, Dec. 1999.
- [7] —, "An explicit dynamic model for direct reforming carbonate fuel cell stack," *IEEE Trans. Energy Conversion*, vol. 16, pp. 289–295, Sept. 2001.
- [8] J. Padullés, G. W. Ault, and J. R. McDonald, "An approach to the dynamic modeling of fuel cell characteristics for distributed generation operation," *J. Power Sources*, 2000.
- [9] K. Schoder, A. Hasanovic, and A. Feliachi, "Load-Flow and dynamic model of UPFC within the power system tool box," in *Proc. Midwest Symp. Circuits Syst.*, Lansing, MI, Aug. 2000.
- [10] L. J. Blomen and M. N. Mugerwa, *Fuel Cell Systems*. New York: Plenum, 1993, pp. 37–69.
- [11] *Fuel Cell Handbook*, 5th ed., EG&G Services Parsons Inc., U.S. Department of Energy, 2000.
- [12] W. He, *Dynamic Simulations of Molten-Carbonate Fuel-Cell Systems*, The Netherlands: Delft Univ. Press, Dec. 2000.
- [13] P. T. Krein, P. Enjati, and J.-S. Lai, *Advanced Fuel Cell Power Conditioning Systems, Fuel-Cell Short Course*. Morgantown, WV: NTU, Mar. 26, 2002.
- [14] K. Schoder, A. Hasanovic, A. Feliachi, and A. Hasanovic, "PAT: A power analysis toolbox for MATLAB/simulink," *IEEE Trans. Power Syst.*, vol. 18, pp. 42–47, Feb. 2003.



Kourosh Sedghisigarchi (S'01) received the Bachelor and Master of Engineering degrees in electrical engineering from Sharif University of Technology, Tehran, Iran, in 1994 and 1997, respectively. He is currently pursuing the Ph.D. degree in the Lane Department of Computer Science and Electrical Engineering Department at West Virginia University, Morgantown, where he is a Graduate Research Assistant.

His research interests include distributed generation, fuel cells, modeling, power distribution systems,

and control.



Ali Feliachi (SM'86) received the Diplôme d'Ingénieur en Electrotechnique from Ecole Nationale Polytechnique of Algiers, Algiers, Algeria, in 1976, and the M.S. and Ph.D. degrees in electrical engineering from the Georgia Institute of Technology, Atlanta, in 1979 and 1983, respectively.

Currently, he is Full Professor and the holder of the endowed Electric Power Systems Chair position in the Lane Department of Computer Science and Electrical Engineering at West Virginia University (WVU), Morgantown, where he has been since

1984. He is also the Director of the Advanced Power and Electricity Research Center at WVU. He has been working in the field of large-scale systems and power systems for 25 years, and has appeared in many publications.

Dr. Feliachi is a member of ASEE, Pi Mu Epsilon, Eta Kappa Nu, and Sigma Xi. He received an ASEE Dow Outstanding Young Faculty Award in 1987, and the following awards from the College of Engineering at WVU: Leadership (1989), Research (1991), and Graduate Teacher (1991), and in 1994, he received the Claude Benedum Distinguished Scholar Award for the Sciences and Technology from WVU.